LAWRENCE
LIVERMORE
NATIONAL
LABORATORY

UCRL-PROC-217271

MRF Applications: Measurement of Process-dependent Subsurface Damage in Optical Materials using the MRF Wedge Technique

J. A. Menapace, P. J. Davis, W. A. Steele, L. L. Wong, T. I. Suratwala, P. E. Miller

November 22, 2005

Boulder Damage Symposium
Boulder, CO, United States
September 19, 2005 through September 21, 2005

This work was performed under the auspices of the U.S. Department of Energy by University of California, Lawrence Livermore National Laboratory under Contract W-7405-Eng-48.

MRF Applications: Measurement of Process-dependent Subsurface Damage in Optical Materials using the MRF Wedge Technique

Joseph A. Menapace*, Pete J. Davis, William A. Steele, Lana L. Wong,
Tayyab I. Suratwala, and Philip E. Miller

University of California, Lawrence Livermore National Laboratory
P.O. Box 808, 7000 East Avenue, L-491, Livermore, CA 94550
925-423-0829 (menapace1@llnl.gov)

Work performed under the auspices of the US Department of Energy by Lawrence Livermore National Laboratory under contract No. W-7405-ENG-48 with the LDRD program.

ABSTRACT

Understanding the behavior of fractures and subsurface damage in the processes used during optic fabrication plays a key role in determining the final quality of the optical surface finish. During the early stages of surface preparation, brittle grinding processes induce fractures at or near an optical surface whose range can extend from depths of a few μm to hundreds of μm depending upon the process and tooling being employed. Controlling the occurrence, structure, and propagation of these sites during subsequent grinding and polishing operations is highly desirable if one wishes to obtain high-quality surfaces that are free of such artifacts. Over the past year, our team has made significant strides in developing a diagnostic technique that combines magnetorheological finishing (MRF) and scanning optical microscopy to measure and characterize subsurface damage in optical materials. The technique takes advantage of the unique nature of MRF to polish a prescribed large-area wedge into the optical surface without propagating existing damage or introducing new damage. The polished wedge is then analyzed to quantify subsurface damage as a function of depth from the original surface. Large-area measurement using scanning optical microscopy provides for improved accuracy and reliability over methods such as the COM ball-dimple technique. Examples of the technique's use will be presented that illustrate the behavior of subsurface damage in fused silica that arises during a variety of intermediate optical fabrication process steps.

Keywords: subsurface damage, MRF, brittle fracture, surface imperfections, laser-induced damage

1. INTRODUCTION

Management of fractures and subsurface mechanical damage (SSD) arising from processes used during optic fabrication plays a vital function in determining the final quality of an optic's surface finish. Brittle grinding processes induce fractures at, or near, an optical surface whose range can extend from depths of a few μm to hundreds of μm[1-5]. These process-induced or process-related fractures not only determine the current state of the optic in the fabrication process, they dictate how much material needs to be removed during subsequent steps[6-8]. The nature and extent of this damage also determines what manufacturing methods will need to be used to ultimately yield a completed optic having a superior surface finish. On the manufacturing floor, lack of knowledge or an insufficient understanding of process-induced fractures all too often leads to insufficient material removal during intermediate fabrication steps. This can result in occurrence of fractures and imperfections in the final optic, can cause the optic to have to be taken backwards in the manufacturing process for rework, or can add time to subsequent fabrication steps, particularly polishing, that reduces productivity and increases costs. From a functional perspective, fractures and SSD ultimately limit the performance of the optic under high stress conditions including high pressure, vacuum, large thermal gradients, and intense laser light. This is particularly important on optics containing flaws that have been hidden beneath a layer of re-deposited and modified material (usually weakly-structured hydrated material)[9]. In this situation, buried SSD can pose a serious problem because of its interaction with the optic's surroundings and sources of activation such as short-wavelength, high-intensity monochromatic light[10].

Over the past year, our team has made significant strides in developing a diagnostic technique that combines magnetorheological finishing (MRF) and scanning optical microscopy to statistically measure and characterize SSD in optical materials. The method is called the MRF Wedge Technique. The technique is deterministic, making it easily controllable in removing a prescribed amount of material from an optical surface. Moreover, it is reproducible and can be applied repeatedly to a high degree of precision with depth and form control to better than 20 nm[6,7]. MRF polishing has also been shown to expose and remove fractures without adding or propagating SSD[8]. This makes it possible for one to evaluate a fabrication step without having to worry about collateral damage from sample preparation or measurement. The MRF Wedge Technique can be applied to large areas on the optic surface that enables one to obtain statistical information on the characteristics of fracture and flaw networks. The method is designed to be used on parts that have been through the same fabrication conditions as parts being produced in a manufacturing line. It also gives information regarding the profile of the fractures moving from the surface into the bulk in addition to the maximum depth of damage in an optic that is at a particular point in the fabrication process. In contrast, other methods, such as the COM ball technique[9], taper polishing method[10], and more recently the MRF spot method[11] suffer from several disadvantages when used to quantitatively examine the statistical distribution of fractures on, or near, an optical surface. First, the interrogations may be restricted to small areas on the optic which limits the acquisition of sufficient information regarding the extent of fractures and SSD actually present over the entire surface. Second, it makes it difficult to easily link the measurements to the process conditions used during fabrication. Third, the methods can be difficult to apply and control to the accuracy needed to measure the extent of damage. Fourth, the material removal scheme used can induce its own SSD to the surface being measured. Lastly, the material removal method (pad or lap polishing, in particular) can move material on the surface and bury fractures making them invisible and difficult, if not impossible, to evaluate.

2. MRF WEDGE TECHNIQUE

The basic concept behind the MRF Wedge Technique is to precisely polish a wedge into the surface of an optic to reveal the fracture network or imperfections present as a function of lateral distance along the wedge. The lateral distance is associated with the depth of the artifacts through knowledge of the wedge contour. This essentially provides information on the fracture distribution present as a function of depth by spreading the distribution laterally along the wedged surface. The MRF Wedge Technique consists of three steps shown in Figure 1. The first step involves obtaining optic specimens representing the manufacturing process needing to be characterized. These specimens can be obtained in a variety of ways. They can be drawn from a specific step of a manufacturing process, such as a particular grinding or polishing operation, as actual work pieces, by using surrogate samples processed in the same manner as production pieces, or they can be cut from actual production work pieces. For the experiments reported in this paper, we found that process-specific fracture networks from grinding and isolated imperfections from polishing can be prepared by adequate material removal during the process being studied or by starting with a polished and well-examined specimen. In the latter case, fractures or imperfections from the process of interest are the only ones present or are the dominant fracture network in the surface. Examples of the MRF Wedge Technique applied to various process-induced specimens are discussed later in this manuscript. These specimens are prepared as follows.

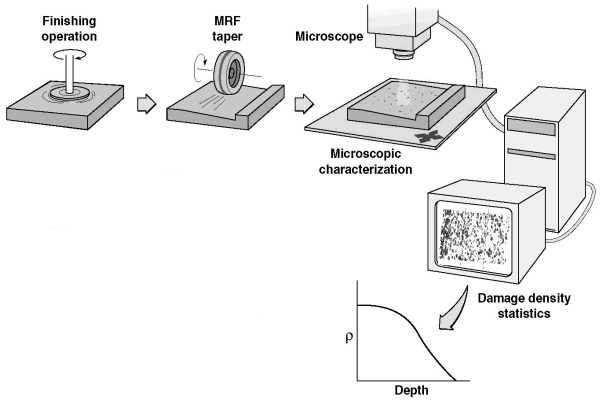

Figure 1: Schematic flow of MRF Wedge Technique used to measure fracture network distributions in optical surfaces. Prepared specimens are wedged polished using the MRF and then analyzed using an automated microscope.

Seven super-polished and MRF processed round fused silica glass (Corning 7980) samples (10 cm diameter × 1.0 cm thick) labeled as Samples A-G were prepared such that they contained no subsurface damage as determined by etching in hydrofluoric acid and inspection. One face of each sample was treated by one of several standard grinding processes. Sample A (Sand blasted) was sand blasted using a Zero Blast-n-Peen Model NPGS-4 sand blasting station

using 300 micron Al2O3 abrasive for 15 minutes. Sample B (120-grit Coarse Blanchard) was generator ground on a Blanchard Model 11A20 grinder using a 120-grit (125 micron) diamond in a metal matrix tool (downward feed rate = 250 μm/min, rotation rate = 45 rpm, time= 20 sec). Sample C (150-grit Coarse Blanchard) was generator ground on a Blanchard Model 11 grinder using a 150 grit (100 micron) diamond in a resin matrix tool (downward feed rate = 230 μm/min, rotation rate = 41 rpm, time= 20 sec). Sample D (15 micron Loose Abrasive) was ground on a Strasbaugh Model 6Y2 grinder using 15 micron Al2O3 abrasive (Microgrit WCA15T) in water on a Pyrex glass lap (load = 25 N, lap rotation rate = 16 rpm, time= 1 hr). Sample E (15 micron Fixed Abrasive) was ground on a Strasbaugh (Model 6DA-DC-2) grinder using 15-micron diamond fixed abrasive in an epoxy matrix (Gator Diamond) (load = 25 N, lap rotation rate = 16 rpm, time= 1 hr). Sample F (9 micron loose Abrasive) was ground on a Strasbaugh Model 6Y2 grinder using 9 micron Al2O3 abrasive (Microgrit WCA9T) in water on a Pyrex lap (load = 25 N, lap rotation rate = 36 rpm, time= 1 hr). Sample G (7 micron Fixed Abrasive) was ground on a Strasbaugh Model 6DA-DC-2 grinder using 7 micron diamond fixed abrasive in an epoxy matrix (Gator Diamond) (load = 25 N, lap rotation rate = 16 rpm, time= 1 hr). After preparation, the samples were developed using wet etching with a 15 minute etch using a 20:1 ammonium fluoride/ hydrofluoric acid solution (commercially known as 20:1 buffered oxide etch). This development method adequately and reproducibly opens fractures at the optical surface that are closed or optically contacted to neighboring material and difficult to observe during microscopic examination[6,7,13,14]. It also exposes subsurface damage generated during the fabrication process that has been subsequently buried under a re-deposited layer of refractive index matched hydrated-glass.

After specimen preparation and development, a Q-22 XY MRF (QED Technologies, Inc.) is used to raster polish a prescribed wedge into the optic side containing the process-induced damage network being evaluated (Figure 1). The lateral dimensions of the polished wedge are 6 cm X 6 cm limited by the diameter of the fused silica specimens used and the need to preserve an area of original surface around the wedge for subsequent reference plane datum generation. In general, any lateral dimension for the wedge can be used and multiple wedges can be placed into the optic surface if multiple experiments need to be conducted. A linear 1-dimensional wedge profile is used to perform the polishing on the MRF because of its simplicity and ease of measurement using the instruments available in the laboratory.

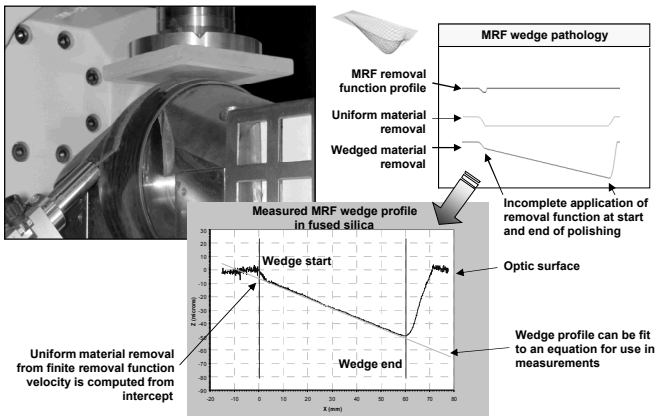

Figure 2: The deterministic nature of the MRF process can accurately polish a wedge into an optical surface. The wedge is imprinted into the surface using a well-defined MRF removal function and computer generated prescription. Surface profilometry is used to measure the surface contour from which mathematical fits are made that correlate lateral contour with depth from the original surface.

Wedge profiles are measured using a Nikon NEXIV VMR series CNC-based optical measuring system. This is done by measuring the surface profile with laser distance measuring interferometry line scans that extend over the polished wedge area with coverage into the surrounding original surface for reference. A typical MRF 1-dimensional wedge profile cross section is shown in Figure 2. The profile shows the details of the wedge which includes the amount of uniform material removal realized from MRF polishing at the start of the taper, the precision of linear portion of the wedge, and the shape of the polished zone after the deepest portion of the wedge is reached. Other wedge profiles such as exponential, fractional power decay, and arbitrary user defined profiles, can be used depending on the depth resolution and signature desired in subsequent analyses. The wedge prescriptions are generated mathematically and converted to an interferogram format using software we developed for imprinting topographical structures onto optical surfaces. The details of this process as well as combining the prescription with a well-defined MRF removal function to polish in the wedge have been previously described[11] and will not be reproduced here. The depth of the MRF polished wedge depends upon the process specimen being evaluated and upon the end point desired. In our experiments, we polished wedges into the specimens to depths beyond where all the process-induced damage is removed. These locations are arbitrarily selected at depths corresponding to approximately three-quarters of the lateral wedge dimension in the direction of increasing depth. Due to the deterministic nature of the MRF process, superposition is used to add to the wedge profiles in iterative MRF

wedge polishing passes. This allows one to continue with wedge polishing in the same area until the appropriate depth for the process specimen is obtained.

The wedged specimens are analyzed using the NEXIV optical measuring system as shown in Figure 3. One major advantage of using this computer-based measuring system is its ability to perform repeated tasks at high speed. This system is located in a vertical laminar flow clean hood (Terra Universal) to minimize contamination from particulates that can accumulate on the surface during examination. Optics being analyzed are placed into a kinematic sample holder that maintains registration of the part in the NEXIV during analysis, particularly if additional polishing passes are made to attain the required wedge depth using the MRF. The sample holder is comprised of two doughnut-shaped aluminum plates, one of which has three equally spaced grooves spaced at 120 degrees cut into its lower surface. The corresponding mating plate has stainless steel ball bearings placed at 120 degrees along a circle centered on the plate. The grooved plate and the optic being studied are glued together using vinyl polysiloxane dental impression epoxy (Examix NDS, GC America, Inc.). The mating plate is attached to the NEXIV. When these plates are placed together during use, accurate and reproducible placement of an optic is attained to less than 2 μm. Accurate and reproducible X-Y placement of the optic is critical to this technique as its goal is to unravel the spatial relationship of imperfections in the specimens as a function of distance along the wedge. The opening in the center of the grooved plate allows the optic to remain in the sample holder during MRF wedge polishing. Vacuum chucks used to hold the optic on the MRF can be inserted into this opening and used to engage the optic onto the spindle during material removal. The NEXIV system is programmed to automatically collect tiled micrographs over a 6 cm X 6 cm area on the optic surface. This area coincides with the wedge area MRF polished into the surface. A complete analysis includes interrogation of about 146,000 tiled micrographs. Images obtained using the NEXIV system are typically collected using episcopic lighting at 150x magnification to resolve surface detail. In our experiments we chose to perform raster tiling across the constant contour areas before stepping to the next deeper contour areas. This strategy minimizes the refocusing required between tiled areas and therefore shortens the time needed for scanning. For each image, we used the laser auto-focus feature on the NEXIV to find the surface before acquiring an image. The NEXIV is programmed to analyze the image before moving to the next location. The analysis consists of applying color space stretching and binary thresholding to each image making surface features black (0, 0, 0 in 24-bit RGB color space) and surrounding "good" material clear, or white (255, 255, 255 in 24-bit RBG color space). The system then singles out the artifacts by location within the image as well as measurements regarding their area, major and minor axis lengths (using a circumscribed ellipse), and major axis orientation away from vertical. This information is written to a file on the NEXIV computer systems for subsequent examination. For most experiments, these characteristics are sufficient to perform data analysis, and therefore, images are not typically saved for each field-of-view to reduce the amount of computer storage space needed. The process is repeated in sequence across and down the wedge until the entire area in analyzed.

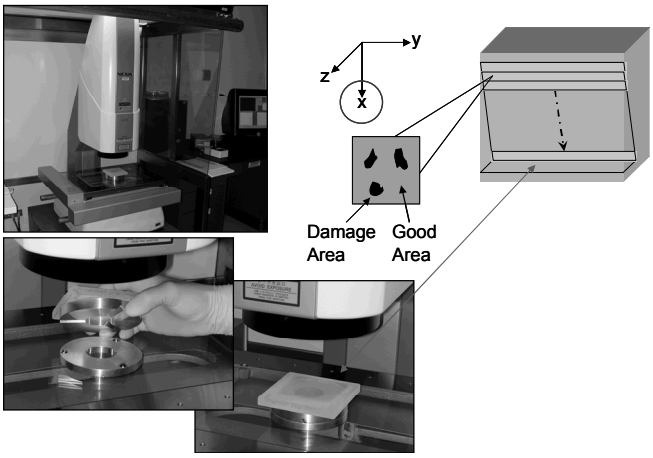

Figure 3: The MRF polished wedge is analyzed using a Nikon NEXIV VMR series CNC-based scanning microscope. The system is maintained in a clean hood to minimize contamination during analysis (top left). A kinematic sample holder is used to accurately and repeatedly register optics on the microscope and MRF spindle (bottom left). Sample analysis is conducted by scanning over the wedged area collecting images that are interpreted and catalogued by a computer system for later interpretation (top right).

The information obtained from the NEXIV analysis is interpreted using software written by the primary author to bin the data into total percent obscuration as a function of wedge depth. Histogram bin widths are derived from the field-of-view dimension in the direction of the wedge contour. An average depth associated with the images position is used to compute position. The depth of the contour at this point is calculated from the wedge profile which is measured and fit to the data (see Figure 2). For each bin, the measured obscuration is summed across the constant contour and subsequently divided by the total bin area analyzed to arrive at total obscuration for that bin. Between 250 thousand and 1 million fractures are typically characterized for the samples using this protocol yielding data reliable down to 1.0×10^{-6} obscuration.

3. ANALYSIS OF PROCESS-INDUCED FRACTURES ON GROUND FUSED SILICA

As an example of the MRF Wedge Technique's application in studying fracture networks, we will summarize the results obtained from analyses conducted fused silica specimens ground using various process types. Figure 4 presents the fracture network distribution as a function of depth from the original surface for the 120-grit coarse Blanchard ground fused silica specimen (Sample B). Overall, the fracture network associated with this grinding process measures in at 75 μm from the original surface. For most of the fracture network profile, the obscuration distribution, shown in the semi-logarithmic plot, appears to follow exponential decay until an abrupt disappearance of the fracture network between 65 and 75 μm in depth. This is consistent with our observations on this specimen when using the 3-dimensional MRF analysis technique[8]. These studies indicate that deeper fractures dominate the network and occur late in time; that is, they most likely occur during the last few rotations of the grinding segments or grinding passes. In comparison, the shallow damage appears to be attributed to deep fractures occurring earlier in time. These fractures are

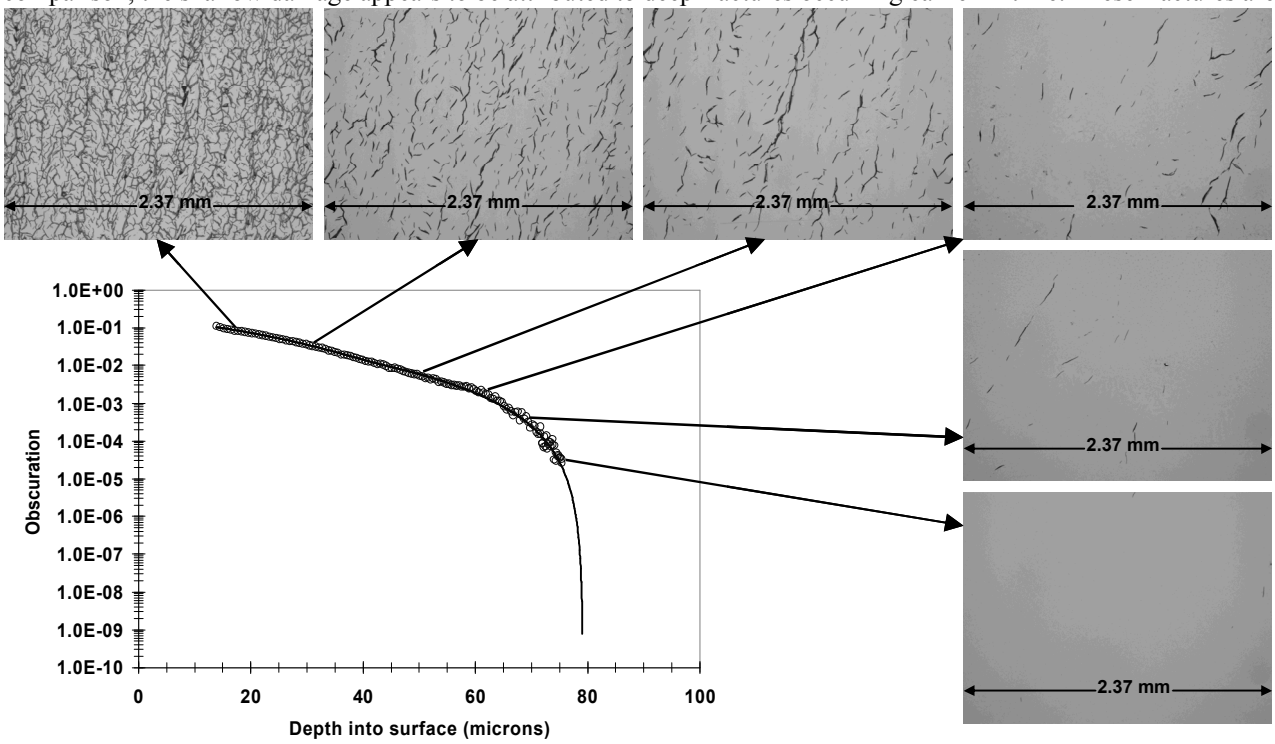

Figure 4: Measured crack depth distribution for a fused silica surface that was ground using a 120-grit fixed abrasive Blanchard process. The plot is shown as a semi-log plot of observed surface obscuration as function of depth from the original surface. Micrographs taken at selected positions on the wedge illustrate the nature of the fracture network and how it changes as the network penetrates into the bulk.

subsequently shortened as the grinding process proceeds and material is removed. The density of the shallow fracture network is higher because they are continuously generated as deep fractures and eventually dominate the surface at shallow depths due to a balance between fracture initiation and material removal. From the micrographs taken at various depths along the MRF wedge, polishing just a few μm into the surface reveals the details of the fracture network arising from this particular grinding process. The rubble zone is removed at about 10 μm into the bulk and a marked decrease in shallow fractures is observed at 20 μm into the bulk. Beyond this point, most of the heavy fracture network is penetrated and the characteristic fracture network for this process dominates. Here, the fracture network which is composed of concatenated fractures of a specific length breaks up into radial fractures possessing a characteristic length. This pattern continues with no or little change in crack length until the network is entirely removed at 75 μm into the bulk. A model explaining this behavior has been developed by our group and is reported elsewhere[7]. Briefly, the model utilizes two major factors that determine the shape of the fracture network distribution. First, the fundamental instantaneous distribution of cracks generated at a particular time at the existing surface and, second, the summation of these fracture distributions and their shortening with continued time and material removal. The model suggests that summation of the fracture profiles formed at each new surface results in an overall

"exponential-like" decay profile except at the ends of the distribution. This profile results regardless of the functional form of fracture distribution occurring immediately at the surface. However, near the end of the distribution where the newest and deepest fractures dominate (low obscuration), the fracture distribution tends to have the shape consistent with the fracture morphology. These fractures are radial in nature and can be represented by high-aspect rounded rectangles openings into the surface; that is, they have flat bottom contour. This results in the disappearance of the network and abrupt decay of the fracture profile observed in the wedged specimens.

Table 1: Maximum fracture depths and characteristic fracture lengths measured in ground fused silica using the MRF wedge Technique.

Specimen	Fracture Depth (μm)	Fracture Length (μm)
Sandblast (Sample A)	131	27
120 grit Generator (Sample B)	79	28
150 grit Generator(Sample C)	42	15
15 μm Loose abrasive(Sample D)	31	4.6
15 μm Fixed Abrasive(Sample E)	18	4.5
9 μm Loose Abrasive(Sample E)	6	2.0
7 μm Fixed Abrasive(Sample G)	28	8.4

The fracture distribution profiles measured for all the ground specimens using the MRF Wedge Technique are summarized in Figure 5. The corresponding maximum statistical fracture depths and lengths for each process are listed in Table 1. Overall, the distributions span 4 to 6 orders of magnitude and follow an exponential decay profile followed by an abrupt cutoff similar to that described above for the 120-grit ground specimen. The results further indicate that the fracture network depths scale, for the most part, with the abrasive size used in the grinding process. This consistent with accepted optical shop protocols where grinding and shaping of an optical surface begins with process steps incorporating large abrasive sizes with subsequent steps using sequentially finer abrasive steps to prepare the surface for polishing. The data also shows that fixed abrasive processes impart less damage to the surfaces than loose abrasives of comparable size. This can be advantageous in process design and selection since fixed abrasive processes also tend to remove material at higher rates than loose abrasive processes. The one exception to this trend is the 7 μm fixed abrasive process. This process possesses an anomalous response when compared to the 9 mm loose abrasive process in that the fracture depth is over 4 times deeper, the fracture length is 4 times longer, and the profile appears to contain scatter below 10^{-3} obscuration. The exact cause of this behavior is unclear; however, we believe that the fixed abrasive (diamonds) used in the pad are too small to be held tightly by the epoxy matrix and are being released during the grinding process as large sharp individual or agglomerated entities. These "contaminants" cause deep fractures as they move across the optic surface and perturb the underlying fracture distribution with anomalous scratches.

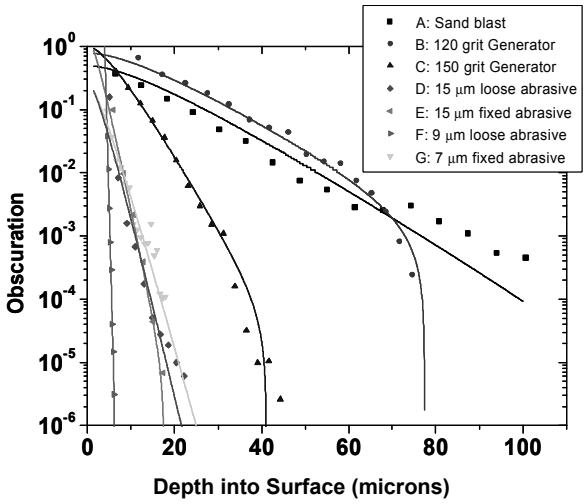

Figure 5: Measured fracture depth distributions for fused silica surfaces that have been treated by a wide variety of grinding processes (Samples A-G).

Selected micrographs taken along the wedged surface for the specimens analyzed are shown in Figure 6. These images correspond to the fracture network morphologies at the indicated depths below the original surfaces. Characteristic fracture patterns and fracture lengths are observed in each of the image sets that are peculiar to the process types and material removal conditions. The sandblasted sample (Sample A) contains characteristic Hertzian impact fractures about 10 times smaller than the grit size used. The cone fractures present on the surface evolve into radial fractures along the wedge. They remain approximately constant in size but decrease in number density until the deepest ones are removed as the fracture depth for this process is attained. The Blanchard ground surfaces (Samples B and C) also contain characteristic fractures running predominantly along the tool segment rotation paths in repeating patterns. The fracture lengths associated with

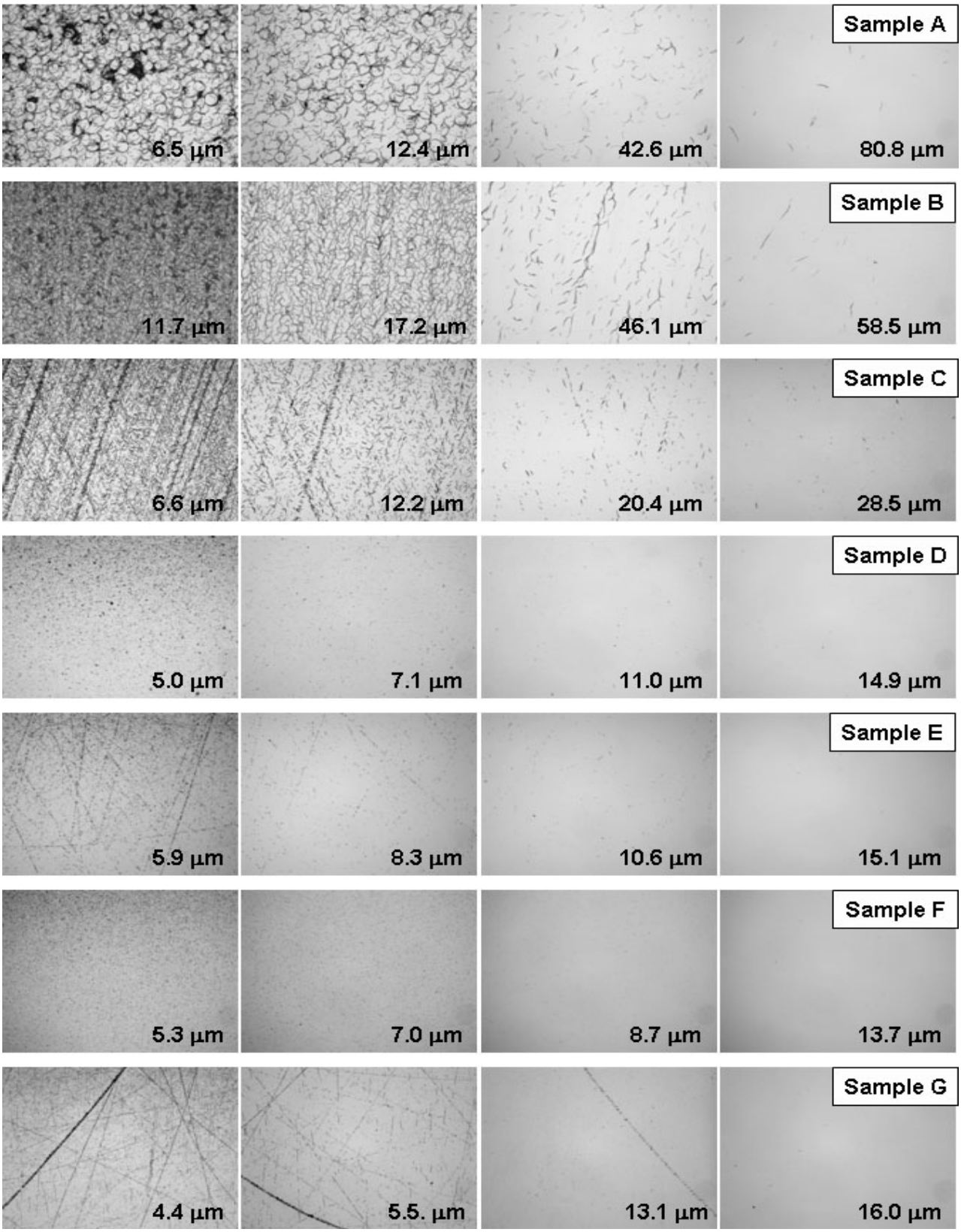

Figure 6: Micrographs collected at selected areas along the MRF polished wedge for fused silica surfaces treated by various grinding processes (Samples A-G). The values in the lower-right corners of each image indicate the depth below the original surface at which the image was taken. The lateral scale for each micrograph is 2.37 mm horizontally.

the two processes are distinct and correlate with the abrasive sizes used. Similar to the case for the sandblasted sample, these fractures possess lengths at about a factor of 10 smaller than the abrasive size. Shortly after polishing through the rubble zone, the fractures induced from the Blanchard process appear to be "trailing" indent type fractures (i.e. chatter marks). These fractures create a mosaic network along the wedge made up of concatenated radial fractures that ultimately separate into the characteristic fracture lengths. The fracture networks for the fixed abrasive ground specimens (Samples E and G) have similar morphological characteristics when compared to the Blanchard ground specimens. They also are composed of trailing indent type fractures with the marked difference being the arbitrary patterning from large abrasive particles randomly embedded in the matrix. For the 15 μm fixed abrasive process, the fracture lengths scale at about 3 times smaller than the abrasive size used. As stated previously, the 7 μm fixed abrasive process has anomalous behavior with respect to its mean abrasive size when compared to either small loose abrasive or 15 μm fixed abrasive processes. This process has a large fracture distribution depth and a fracture length about the same as the mean abrasive size. The images further suggest that a few larger size abrasive particles are responsible for the dominant fracture network. The loose abrasive ground samples (Samples D and F) possess entirely different fracture morphologies when compared to the fixed abrasive processes. The fracture networks in these cases consist of randomly positioned trailing indent type fractures with little to no long range morphology. This can be attributed to the highly random nature of the loose abrasive process and the ability for abrasive to freely move over the optical surface during grinding.

5. SUMMARY AND CONCLUSIONS

The MRF Wedge Technique has been shown to be a valuable tool when used to study the details of fracture networks and imperfections in optical materials. We have demonstrated the technique in experiments yielding direct observation of the fracture depth and length distributions present in various common grinding processes. The measurements conducted on the various grinding processes indicate that the fracture networks are unique to each process and can not be estimated with certainty given "general optical shop rules". For example, one common rule in the optical ship recommends that the amount of material that needs to be removed in a process should be roughly 3 times the abrasive particle size. The depth and length of the fractures are strongly correlated with a given process. Taking a minute to study Table I will lead one to conclude that too much or too little material would be removed if one uses a general rule. As far as production is concerned, this leads to inefficiency on one hand, and more severely, fabricating optics containing damage in the other. The MRF Wedge Technique enables one to characterize each step in the fabrication process and to design and optimize process steps which may lead to more cost effective processes and higher quality optics. This method of material removal and characterization has enabled us to gain an understanding of how optical fabrication processes interact with an optical surface and has led us to an understanding of how to optimize the optical fabrication process so that higher quality optics can be manufactured using the best known methods and material removal protocols. Our experience in conventional finishing suggests that every process used to fabricate an optic imparts some level of damage at, or near, the surface. Detailed knowledge of the required material removal at each step is a necessary condition to avoiding damage propagation into subsequent process steps or damage "pile up" in a finished optic from processes early in the fabrication protocol. This knowledge needs to cover the entire fabrication process from blank to finished optic. The MRF Wedge Technique can be used to understand issues with processes under development by providing information on the fracture networks present as well as their depths. It enables one to directly observe and distinguish artifacts such as scratches or fractures arising from extrinsic events, such as mishandling, from intrinsic issues, such as abrasive particle or lap contamination. Specimens and the data collected during characterization can also be used to troubleshoot process steps in production. They provide a baseline on how the process performs when working properly and, when compared to specimens processed during periods of difficulty, they can help point to how much the process characteristics have changes and may point to a root cause of the problem.

REFERENCES

1. T. Kamimura, S. Akamatsu, H. Horibe, H. Shiba, S. Motokoshi, T. Sakamoto, T. Jitsuno, T. Okamoto, and K. Yoshida, "Enhancement of Subsurface-Damage Resistance by Removing Subsurface Damage in Fused Silica and Its Dependence on Wavelength", *Japanese Journal of Applied Physics*, **43, 9A/B**, 1229-1231 (2004).
2. T. Yoshino, Y. Kurata, Y. Terasaki, and K. Susa, "Mechanisms of polishing of SiO_2 films by CeO_2 particles", *Journal of Non-Crystalline Solids*, **283**, 129-136 (2001).
3. D. W. Camp, M. R. Kozlowski, L. M. Sheehan, M. Nichols, M. Dovik, R. Raether, I. Thomas, "Subsurface damage and polishing compound effect at the 355-nm laser damage threshold of fused silica surfaces", *Laser Induced Damage in Optical Materials, SPIE Proc*., **3244**, 356-364 (1997).
4. N. Brown, "Optical Fabrication", *Lawrence Livermore National Laboratory Report* , MISC 4476, August 1989.
5. F. Preston, "Structure of abraded surface glasses", *Trans. Opt. Soc.,* **23(3)**, 141-162 (1922).
6. P. E. Miller, T. I. Suratwala, J. P. Menapace, L. L. Wong, P. J. Davis, and W. A. Steele, "The Distribution of Subsurface Damage in Fused Silica" *Laser Induced Damage in Optical Materials,* this proceedings, Boulder, Co (2005).
7. T. Suratwala, L. Wong, P. Miller, M. D. Feit, J. Menapace, R. Steele, P. Davis, D. Walmer, "Sub-surface mechanical damage distributions during grinding of fused silica", *Journal of the American Ceramics Society*, in submission.
8. J. A. Menapace, P. J. Davis, W. A. Steele, L. L. Wong, T. I. Suratwala, and P. E. Miller, "Utilization of Magnetorheological Finishing as a Diagnostic Tool for Investigating the Three-Dimensional Structure of Fractures in Fused Silica", *Laser Induced Damage in Optical Materials,* this proceedings, Boulder, Co (2005).
9. G. Beilby, "Aggregation and Flow of Solids", 1st Ed, London: Macmillan and Co. (1921).
10. E. Moses, J. Campbell, C. Stolz, C. Wuest, SPIE **5001** (2003) 1.
11. J. A. Menapace, S. N. Dixit, Francois Y. Génin, and W. F. Brocious, "Magnetorheological Finishing for Imprinting Continuous Phase Plate Structure onto Optical Surfaces", *Laser Induced Damage in Optical Materials, SPIE Proc*., **5273**, 220-230 (2003).
12. S. D. Jacobs, D. Golini, Y. Hsu, B.E. Puchebner, D. Strafford, W. I. Kordonski, I. V. Prokhorov, E. Fess, D. Pietrowski, and V. W. Kordonski," Magnetorheological finishing: a deterministic process for optics manufacturing", *SPIE*, **2576**, 372-382 (1995).
13. J. A. Menapace, B Penetrante, D. Golini, A. Slomba, P. E. Miller, T Parham, M Nichols, and J. Peterson, "Combined Advanced Finishing and UV-Laser Conditioning for Producing UV-Damage-Resistant Fused Silica Optics", *Laser Induced Damage in Optical Materials, SPIE Proc*., **4679**, 56-67 (2002). U.S. Patent No. 6,920,765 B2.
14. Y. Zhou, P. Funkenbusch, D. Quesnel, D. Golini, and A. Lindquist, "Effect of etching and imaging mode on the measurement of subsurface damage in microground optical glasses" J. Amer. Ceram. Soc. 77 (1994) 3277-3280.
15. P. Hed, D. Edwards "Optical glass fabrication technology. Relationship between surface roughness and subsurface damage", Applied Optics 26:21 (1987) 4677.
16. J. Randi, J. Lambropoulos, S. Jacobs, "Subsurface damage in some single crystalline optical materials" Applied Optics 44(12) (2005) 2241-2249.